

1 **Fine scale plant community assessment in coastal meadows using UAV based**
2 **multispectral data**

3 **Villoslada Peciña, M.⁽¹⁾, Bergamo, T.F.⁽¹⁾, Ward, R.D.^(1,2), Burnside, N.G.⁽²⁾, Joyce, C.B.⁽²⁾, Bunce, R.G.H. ⁽¹⁾ Sepp,**
4 **K.⁽¹⁾**

5 1) Institute of Agriculture and Environmental Sciences, Estonian University of Life Sciences, Kreutzwaldi
6 13 5, EE-51014 Tartu, Estonia.

7 2) Centre for Aquatic Environments, School of the Environment and Technology, University of Brighton,
8 Cockcroft Building, Moulsecoomb, Brighton, BN2 4GJ, United Kingdom

9
10 Corresponding author: Miguel Villoslada

11 mpecina@emu.ee

12 Kreutzwaldi 5, room 2c18, Tartu, 51014, Estonia

13

14 **Highlights:**

- 15 - Plant communities in coastal wetlands are at risk due to the impacts of global change
- 16 - Knowing the distribution of plant communities is essential for nature conservation
- 17 - Communities distribution maps were produced using a UAV-based multispectral sensor
- 18 - The Random Forest classifier yielded the highest classification accuracy
- 19 - Species diversity and aboveground biomass affect the classification performance

20

21 **ABSTRACT**

22 Coastal meadows worldwide are subjected to habitat degradation due to abandonment,
23 intensification and the impacts of global change. In order to protect and restore these habitats and
24 ensure the supply of valuable ecosystem services, it is necessary to know the extent and location of
25 plant communities in coastal meadows. In this study, five plant communities were mapped at very high
26 resolution in three different study sites in West Estonia. A fixed wing UAV was used to obtain
27 multispectral images and derive a set of vegetation indices. Two different image classification
28 techniques were used to cluster the vegetation indices maps and produce plant community
29 distribution maps. The highest classification accuracy was obtained using a Random Forest classifier
30 and 13 vegetation indices. Additionally, the spectral characteristics of the training samples were
31 correlated with aboveground biomass and species diversity. Both biomass and species diversity were
32 positively correlated with the spectral diversity of training samples and are thus likely to have an effect
33 on the classification accuracy. The results of this study highlight the need to utilize a wide array of
34 vegetation indices and assess the spectral characteristics of training samples in order to obtain high
35 classification accuracies and understand the nature of misclassification errors. The resulting maps
36 provide a solid foundation for global change impact assessment and habitat management and
37 restoration in coastal meadows.

38

39 **KEYWORDS**

40 Coastal plant communities; UAV; vegetation indices; Random Forests; unsupervised classification

41 1. INTRODUCTION

42 Biodiversity loss is a worldwide concern due to impacts from a variety of anthropogenic factors
43 (Cardinale et al., 2012), and climate and land-use change are principal threats to vegetated coastal
44 ecosystems and their supporting biodiversity (IPCC, 2013; Newbold et al. 2016). These threats include
45 sea level rise, increasing storminess, changes in salinity (Ward et al. 2016b) and changes to
46 management regimes, particularly for coastal plant communities (Clausen et al., 2013). In the Baltic
47 Sea Region, Boreal Baltic coastal meadows are European priority habitats (EU Habitats Directive, 1992)
48 resulting from continuous, low-intensity management, in the form of grazing and mowing (Paal, 1998).
49 These grasslands support characteristic plant species and provide a habitat for a diversity of migratory
50 and breeding bird species (Söderström et al. 2001) as well as a variety of plant species on the edge of
51 their ranges (Paal, 1998). They also provide a wide range of ecosystem services including: fodder for
52 cattle, carbon storage, habitat for pollinators, habitat for breeding and migratory birds, erosion
53 control, and flood regulation (Leito et al., 2014; Villoslada et al., 2019)

54 In spite of their ecological importance, coastal meadows have been subjected to habitat degradation
55 in the form of agricultural intensification in many areas and abandonment in others (Henle et al., 2008)
56 and will likely be impacted by global change (Ward et al., 2016b). Whilst efforts have been made in
57 some regions to halt this trend there is limited data available as to the current location and extent of
58 the plant communities in many areas, and as a result there is little underlying information to support
59 nature protection, restoration and management strategies.

60 In these coastal ecosystems, the provision of ecosystem services and resilience to environmental
61 stressors including climate change are largely dependent on plant community type. In this regard,
62 communities can be used as an indicator that can highlight environmental gradients (Ellenberg, 1979;
63 Diekmann, 2003; Berg et al., 2012; Ward et al., 2013; 2016a) and can also be used to elucidate
64 management status, disturbance or abandonment (Burnside et al., 2007; Brotherton & Joyce, 2015)
65 and the impacts of management regimes and intensity (Joyce, 2014; Joyce et al., 2016). Plant
66 community classification is a well-established tool in ecology (Tansley, 1920; Mueller-Dombois &
67 Ellenberg, 1974; Crawley, 1997; Burnside et al., 2007) and plants are often used as indicators due to
68 the fact that they are relatively simple to survey and can give a powerful overview of the ecosystem.
69 Moreover, in the frame of ecosystem services (ES) science and practice, plant communities can be
70 regarded as Service Providing Units (SPUs) , understood as spatially explicit units within which ES are
71 provided (Burkhard & Maes, 2017). SPUs constitute an essential first step to obtain robust ecosystem
72 service supply models because they reflect the underlying ecosystem functions and their spatially
73 explicit nature (Crossman et al., 2013). In this respect, recent methodological developments for
74 mapping and assessment of ecosystem functions and services require very detailed spatial and
75 thematic scales to model the complex dynamics of ecosystem service supply (Zulian et al., 2018).
76 However, data concerning the location and extent of plant communities over large scales is often costly
77 and time consuming to acquire. This problem has been in part addressed through the increased use of
78 GIS and remotely sensed data (Jensen, 2007).

79 With the advent and rapid development of GIS software and the large amount of remotely sensed data
80 available, these tools have been increasingly used for predictive plant community mapping (Burnside
81 & Waite, 2011). Among the wide range of remote sensing techniques and platforms, there are many
82 studies that use passive multispectral remotely sensed data to identify plant communities (Townsend
83 & Walsh, 2001; Brown et al., 2006; Balzarolo et al., 2009; Berni et al., 2009; Hamada et al., 2011; Strong
84 et al., 2017). These studies used a methodology based on identifying specific reflectance values in
85 different wavelengths of distinct vegetation by performing some form of classification, either
86 unsupervised or supervised (Jones & Vaughn, 2010).

87 Satellite imagery has proven useful for automated or semi-automated vegetation mapping at a variety
88 of scales, from regional level and low spatial resolution (Armitage et al., 2015) to community-level and
89 high spatial resolution (Davidson et al., 2016). However, the sometimes coarse spatial resolution of
90 these products render them impracticable for detailed plant community mapping, particularly within
91 grasslands due to the fine scale pattern of communities (Rocchini et al., 2015). On the contrary, the
92 availability and use of Unmanned Aerial Vehicles (UAVs) has undergone an exponential increase during
93 the last decade (Baena et al., 2018). UAVs equipped with consumer grade digital cameras (Rasmussen
94 et al., 2016), multispectral sensors (Candiago et al., 2015), hyperspectral sensors (Aasen et al., 2015)
95 and thermal sensors (Turner et al., 2018) have been used in fields such as ecology, forestry, nature
96 conservation and precision agriculture (Adão et al., 2017; Veettil et al., 2019), providing a much more
97 detailed spatial resolution, in most cases down to the centimetre-scale. At the same time, the
98 increasing amount of remotely sensed data produced with different satellite platforms and UAVs poses
99 a challenge in terms of data processing and classification (Adão et al., 2017). Unsupervised and
100 supervised classification algorithms are therefore a crucial tool to achieve interpretable results.

101 Unsupervised classification techniques group pixels according to their similarity in feature distance
102 using a variety of different algorithms. Unsupervised classification does not require information on the
103 spectral signatures of the objects under study. Instead, unsupervised classification methods cluster
104 multidimensional datasets into relatively homogeneous classes of similar spectral signatures (Duda &
105 Canty, 2002). A wide array of unsupervised algorithms have been used in diverse applications,
106 including automated mapping of tree species diversity (Schäfer et al, 2016), individual plant species
107 mapping (Everitt et al, 2015) and environmental stratifications (Villoslada et al, 2016). However, a
108 major drawback to this methodology is that the classes do not necessarily relate to different plant
109 community classes on the ground, although the method does provide a good overview of spectral
110 differences over the whole dataset (Jones & Vaughn, 2010).

111 Supervised classification on the other hand, uses training sample areas to direct the classification
112 process. Training sample areas can relate to plant communities or habitat data and are used to classify
113 across the image (Hamada et al., 2011). These training pixels can be used to provide an accurate
114 prediction of the location of different plant communities. A lot of attention has been directed towards
115 the number of training samples and the size of training polygons (Chen & Stow, 2002). However, the
116 spectral characteristics of training samples may also have an effect on the classification performance.
117 According to the Spectral Variation Hypothesis, the spectral variability of remotely sensed images is
118 defined as the spatial variability of the remotely sensed signal within a given area and directly related
119 to plant community type and species diversity (Rochinni et al, 2004). Previous studies (Oldeland et al,
120 2010; Rochinni et al., 2010b; Medina et al., 2013; Cavender-Bares et al., 2017), have assessed the
121 relationship between ecological diversity at different scales and the spectral properties of the
122 ecosystems under study. At the field/local scale, remote sensing has been proposed as a tool to
123 estimate environmental heterogeneity and species diversity (Rochinni et al, 2010a). Grassland
124 morphological characteristics, including biomass production, are also likely to affect spectral
125 reflectance (Schweiger et al., 2018). Although spectral heterogeneity shows promising results in the
126 fields of biodiversity monitoring and habitat management, it should also be accounted for in relation
127 to the characteristics and quality of spectral training samples used in supervised algorithms. In order
128 to adequately reveal the effects of species diversity on the spectral variability of the studied plant
129 communities and its impact on classification, a pixel-based classification algorithm was preferred over
130 an object-based image analysis classifier (OBIA). OBIA uses a set of features beyond pixel spectral
131 information, namely shape, texture and context (Liu & Xia, 2010). Although OBIA is considered to be a
132 superior classification technique (Blaschke, 2010), the effects of shape, texture and context on the

133 classification performance may interfere with the spectral variability analysis and was therefore
134 discarded.

135 Among the wide spectrum of classifiers, the Random Forest machine learning classifier (Breiman, 2001)
136 has been broadly used in recent years to extract information from multispectral, hyperspectral, radar,
137 LiDAR and thermal imagery (Belgiu & Drăguț, 2016) as a powerful and efficient classification technique.
138 Random Forest (RF) is an ensemble learning technique that has higher accuracy and is less impacted
139 by the effects of noise compared to other machine learning algorithms that use single classifiers
140 (Dietterich, 2000). This machine learning technique presents many advantages for remote sensing as:
141 it runs efficiently on large databases; it estimates what variables are important in the classification;
142 and it can deal with the nonlinearity of variables (Breiman, 2001; Gislason et al., 2006). Random Forest
143 is based on decision trees, which enable the simultaneous classification of features based on a set of
144 training samples and determination of the best performing explanatory variables (a bagging approach)
145 (Lu & He, 2017).

146 Despite its great potential and recent progress, the use of UAVs and classification algorithms for
147 mapping grassland plant communities has received little attention in the scientific literature. Some
148 studies have utilized different sensors and statistical algorithms to automatically map grassland
149 communities, from consumer grade cameras (Gonçalves et al., 2015; Lu & He, 2017) to multispectral
150 sensors (Strong et al., 2017). In addition, UAVs have been used to estimate aboveground biomass
151 production in grasslands (Wang et al., 2017).

152 In order to address the lack of knowledge and data on the location, spatial configuration and extent of
153 plant communities in coastal meadows, the aim of this study was to assess the potential of UAVs and
154 multispectral cameras for classifying and fine scale mapping of plant communities in coastal meadows.
155 The objectives were to: (1) derive a wide range of vegetation indices from multispectral images and
156 assess their capacity to differentiate between five plant community types in coastal meadows; (2)
157 assess the capacity of supervised and unsupervised classification methods to differentiate between
158 five plant community types and compare the results in a spatially explicit manner; (3) assess the
159 spectral characteristics of training samples in relation to plant community composition and
160 aboveground biomass.

161

162 2. MATERIALS AND METHODS

163 2.1. STUDY SITES

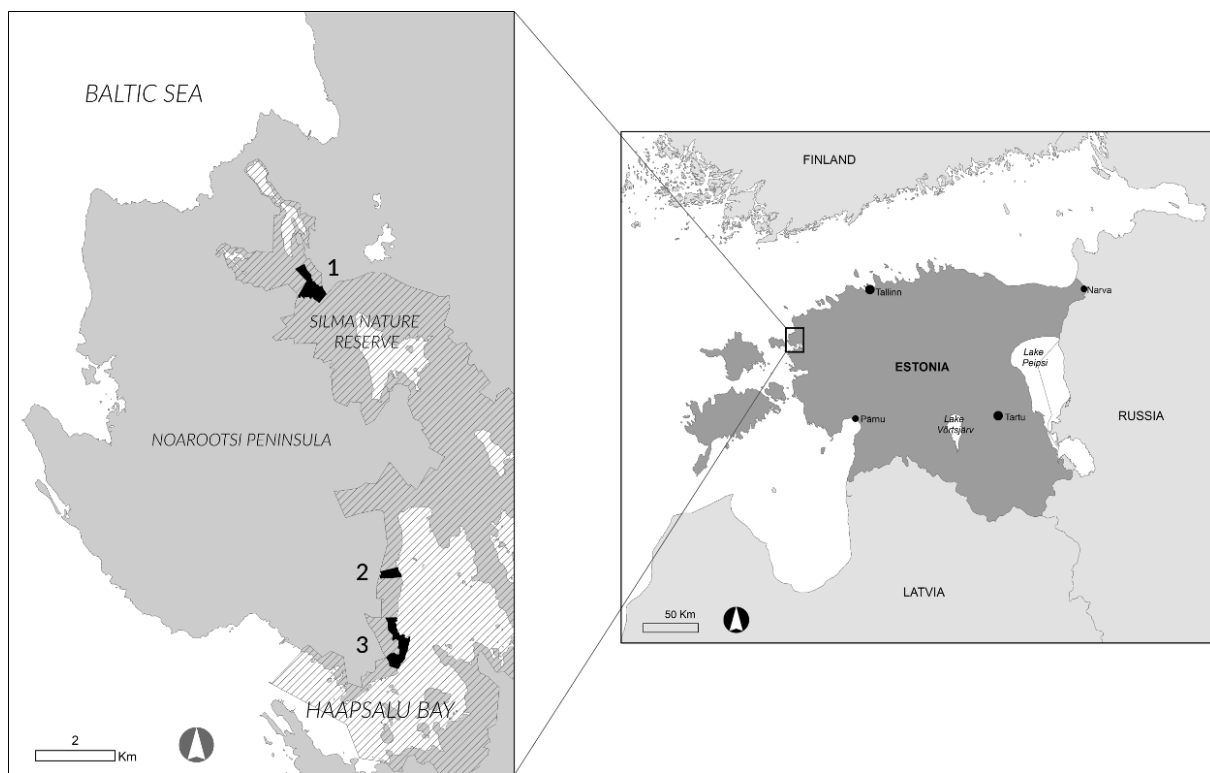
164 Estonia is located in the Baltic region between Latvia, Russia and Finland, in the border between the
165 Boreal and Nemoral zones (Metzger et al., 2005). Despite its relatively small size (45228 km²) Estonia
166 exhibits a high geological, morphological, and climatic diversity (Arold, 2005) and a long coastline of
167 3794 km due to the abundant bays, peninsulas, islands and islets (Ward, 2012).

168 Among the various coastal habitats in Estonia, coastal meadows (classified as Boreal Baltic coastal
169 meadows according to Annex I of the Habitats Directive) occur in sheltered bays and coastlines and
170 are characterised by low relief, often not exceeding a maximum elevation of 2m above mean sea level
171 (Ward et al., 2016b). Baltic coastal meadow landscapes typically consist of coastal wet grasslands, with
172 swamp vegetation on the seaward edge, and scrub vegetation on the landward side. Baltic coastal
173 meadows are formed and maintained by isostatic uplift/sediment accretion (Ward et al., 2014) and
174 regular management, usually in the form of low intensity grazing or mowing (Berg et al., 2012). This
175 low intensity human intervention halts succession to coarser vegetation types such as scrub, woodland

176 and reed swamp and promotes high species richness (Burnside et al., 2007). As a result of habitat
 177 degradation coastal meadows have undergone a considerable loss of area, from 28 750 ha of managed
 178 meadows in the 1950s (EFN & RDSFNC, 2001) to around 8 000 ha in the 2000s (Ingerpuu & Sarv, 2015).

179 This study was undertaken in the Silma Nature Reserve in West Estonia. The reserve covers an area of
 180 4780 ha and encompasses around 560 ha of coastal meadow (Burnside et al., 2007). Landowners
 181 include both the state and private persons. Silma Nature Reserve was first designated as a protected
 182 area in 1998 due to its strategic location along European bird migratory routes (Ward, 2012). Within
 183 the Reserve, three coastal meadows were selected for the analysis: Tahu North, Tahu South and Kudani
 184 (**Fig.1**). The sites were chosen due to the representability of the plant communities they contain and
 185 the continuous management undertaken since the 1990s. The three sites are regularly grazed with
 186 densities of 0.4 – 1.3 Au/ ha according to the data registered by the Estonian Agricultural Registers and
 187 Information Board and the Silma Nature Protection Area Management Plan (Keskonnaamet, 2017).

188



189

190 **Fig. 1.** Location of the study sites within the Silma Nature Reserve in West Estonia: (1) Kudani, (2) Tahu
 191 North, (3) Tahu South.

192 The vegetation at the study sites has been previously categorized into seven plant communities
 193 according the phytosociological classification developed by Burnside et al. (2007): Reed swamp (RS),
 194 Clubrush swamp (CS), lower shore meadow (LS), upper shore meadow (US), open pioneer (OP), tall
 195 grass (TG) and Scrub and developing Woodland (SW). Because of their peripheral occurrence in coastal
 196 meadows, the present study excludes CS and SW from the analysis. Table 1 contains a summary of the
 197 indicator species of the selected plant communities.

198 **Table 1:** Indicator species of selected plant communities. Adapted from Ward et al. (2016b).

Community	Key Species
Reed Swamp (RS)	<i>Phragmites australis</i>

Lower Shore (LS)	<i>Juncus gerardii</i> , <i>Plantago maritima</i>
Upper Shore (US)	<i>Festuca rubra</i> , <i>Leontodon autumnalis</i>
Open Pioneer (OP)	<i>Salicornia europaea</i> , <i>Suaeda maritima</i>
Tall Grass (TG)	<i>Elytrigia repens</i> , <i>Festuca arundinacea</i>

199

200

201 2.2. DATA COLLECTION

202 2.2.1 Plant community field sampling

203 Field sampling was undertaken in July 2018 over a 1 week period. Plant communities were identified
 204 based on the phytosociological key developed for Baltic coastal wetlands (Table 1; Burnside et al.,
 205 2007).

206 In total, 140 1m² quadrats were located using a stratified random approach (ten quadrats per
 207 community type in three sites) (Ward et al., 2016b). Within the quadrats, plants with an area coverage
 208 of 5% or more were recorded (Rodwell, 1995), as well as the cover of bare ground and litter. In the
 209 Open Pioneer community all plants were recorded as a result of the low cover of all species and
 210 predominance of bare ground.

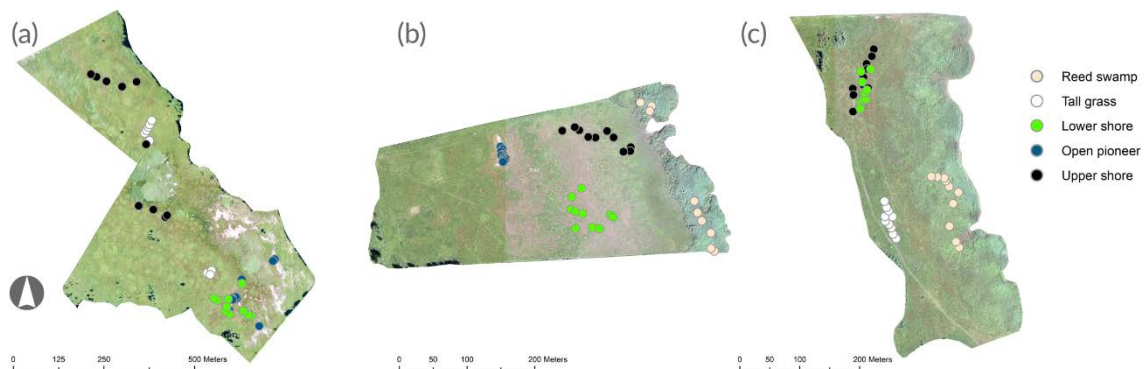
211 X, Y and Z coordinates were recorded within all quadrats using a Sokkia GSR2700 ISX dGPS. Points were
 212 recorded in the corners and centre of all quadrats, five points per quadrat (Ward et al., 2013).

213 At Kudani, Lower Shore, Upper Shore, Open Pioneer and Tall Grass, plant communities were recorded.
 214 At Tahu North, Reed Swamp, Lower Shore, Upper Shore and Open Pioneer were recorded. And at Tahu
 215 South, Reed Swamp, Lower Shore, Upper Shore and Open Pioneer were recorded (Fig. 2). These were
 216 selected based on the plant communities that occurred in each site.

217 Additionally, aboveground biomass samples were collected at each study site in order correlate
 218 communities' structure with the spectral characteristics of the sampling quadrats. A 30 x 30 cm
 219 biomass sampling plot was randomly placed within each vegetation quadrat after the species cover
 220 had been recorded. Grass was cut at ground level and samples were subsequently dried at 80°C for
 221 48h and weighed. Reed Swamp was excluded from the biomass analysis due to logistical constraints.

222

223



224

225 **Fig. 2.** Location of the sampling quadrats within the three study sites: (a) Kudani, (b) Tahu North, (c)
226 Tahu South.

227 2.2.2 Image acquisition

228 Multispectral images were collected using a senseFly Ebee fixed wing UAV, with real-time kinematic
229 (RTK) correction. The images were captured at a flight height of 120 metres, with a 10 cm pixel
230 resolution. A Parrot Sequoia 1.2 megapixel monochromatic multi-spectral sensor was used to collect
231 four distinct spectral bands: Green (530–570 nm), red (640–680 nm), red edge (730–740 nm) and near
232 infrared (770–810 nm). Prior to each flight, an Airinov radiometric calibration target was used to
233 capture calibration images for subsequent radiometric correction of the multispectral images. The
234 images were captured during a total of five separate flights over the three coastal meadow sites
235 covering an overall flight area of 61.4 ha.

236 Eleven ground control points (GCPs) were recorded using a Sokkia GSR2700 ISX dGPS for each flight in
237 order to assess the geopositioning accuracy of the multispectral images (Strong et al. 2017).

238

239 2.3. IMAGE PROCESSING AND ANALYSIS

240 A total of 7615 images were pre-processed in eMotion 3[®]. RINEX observation and navigation files were
241 obtained from the ESTPOS Estonian GNSS-RTK permanent stations network (Eesti Maa-amet) for the
242 post-processed kinematic (PPK) corrections of the images in eMotion 3[®]. This process ensures a
243 significant increase in the positional accuracy of the multispectral images (Tadowski, 2014), from ca.
244 5 m to under 7 cm in the present study.

245 In order to obtain one multispectral orthomosaic per study site, the images were processed in Pix4D
246 v.4.3.31[®]. The orthomosaics were subsequently clipped to the extent of the study sites in order to
247 avoid the interference of the surrounding forest and scrub in the classification of the meadow
248 vegetation.

249 The accuracy of the PPK corrections was assessed through Root Mean Square Error (RMSE) and Mean
250 Absolute Error (MAE) calculations. RMSE and MAE were used to estimate the differences between the
251 GCPs location in the images and the independent GCPs locations measured with the dGPS (Strong et
252 al., 2017).

253 2.4. VEGETATION INDICES

254 A number of vegetation indices have been selected in the present study in order to determine their
255 ability to differentiate plant community types. Satellite-derived vegetation indices have been used
256 since the 1970s to gather information on vegetation health status, forest biomass production,
257 agricultural production and crop monitoring and biodiversity conservation among other applications.
258 The most commonly used vegetation index is the Normalized Difference Vegetation Index (NDVI)
259 (Rouse et al., 1974). Originally conceived as an index to identify vegetated areas and assess their
260 photosynthetic activity, the use of NDVI has been extended to a wide range of fields such as precision
261 agriculture (Houberg & McCabe, 2016), forestry (Robinson et al., 2017), fire damage assessment
262 (Navarro et al., 2017) and habitat monitoring (Mafi-Gholami et al., 2019). Later, a wide variety of
263 vegetation indices have been developed that partly overcome NDVI's limitations (Gu et al., 2013; Xue
264 & Su 2017). Among the indices selected for this study, some incorporate the red-edge region (680 –
265 750nm) in their formulation, which is highly sensitive to leaf area index (LAI) and chlorophyll content

266 and shows high potential for discerning vegetation characteristics and stress factors, as well as
 267 distinguishing plant community types (Delegido et al., 2013).

268 Table 2 contains the 13 indices selected for the study and the corresponding references. The selection
 269 of indices was undertaken based on their specific application in vegetation studies, as each individual
 270 index targets different aspects of vegetation condition, phenology, primary production and vegetation
 271 structure among others.

272

273 **Table 2.** List of vegetation indices selected in the present study. Vegetation indices were used to
 274 classify and map plant communities in the three coastal meadow sites.

Vegetation index	Equation	Reference
Normalized Difference Vegetation Index (NDVI)	$(NIR-R)/(NIR+R)$	Rouse et al. (1974)
Green Difference Vegetation Index (GDVI)	$NIR-G$	Sripada et al. (2006)
Green Normalized Vegetation Index (GNDVI)	$(NIR-G)/(NIR+G)$	Gitelson et al. (1996)
Green Ratio Vegetation Index (GRVI)	NIR/G	Sripada et al. (2006)
Green Infrared Percentage Vegetation Index (GIPVI)	$NIR/(NIR+G)$	Crippen (1990)
Simple Ratio (SR)	NIR/R	Jordan (1969)
Green Difference Index (GDI)	$NIR-R+G$	Gianelle and Vescovo (2007)
Green Red Difference Index (GRDI)	$(G-R)/(G+R)$	Gianelle and Vescovo (2007)
Red edge normalized difference vegetation index (NDVI _{re})	$(NIR-Rededge)/(NIR+Rededge)$	Gitelson and Merzlyak (1994)
Red edge simple ratio (SR _{re})	$NIR/Rededge$	Gitelson and Merzlyak (1994)
Red edge triangular vegetation index (core only) (RTV _{core})	$100(NIR-Rededge)-10(NIR-G)$	Chen et al. (2010)
MSR _{red edge}	$(NIR/Rededge)-1/\sqrt{(NIR/Rededge)+1}$	Wu et al. (2008)
Datt4	$R/G*Rededge$	Datt (1998)

275

276

277 2.5 SUPERVISED PLANT COMMUNITY CLASSIFICATION

278 In order to automatically classify and map plant communities in coastal meadows, a supervised
 279 classifier algorithm was used to generate plant community maps for the study sites. The classification
 280 of plant communities was performed in R (v3.5.1) using a Random Forest machine learning classifier.

281 R packages used to perform RF were:

- 282 • rgdal package: provides bindings to the Geospatial Data Abstraction Library (GDAL) to be
283 imported into R (Bivand et al., 2015)
- 284 • raster package: enabling to read, manipulate, analyze and model the gridded spatial data
285 (Hijmans & van Etten, 2012).
- 286 • caret package: contains functions to streamline the model training process for complex
287 regression and classification problems, and estimate model performance from a training dataset
288 (Kuhn, 2012).
- 289 • randomForest package: for classification and regression based on a forest of decision trees
290 using random inputs (Liaw & Wiener, 2002).
- 291 • e1071 package: contains functions for latent class analysis and shortest path computation
292 (Dimitriadou et al., 2006)

293 The Random Forest classifier was run with all the vegetation indices calculated in the previous step. All
294 pixels falling within each of the 140 sampling quadrats were assigned to the corresponding plant
295 community identified in the field and utilized as the training dataset. Additionally, plant community
296 type was recorded in a supplementary batch of 140 quadrats as a validation dataset.

297

298 2.5 UNSUPERVISED PLANT COMMUNITY CLASSIFICATION

299 In order to explore the capabilities of different image classification techniques, the original dataset
300 composed of 13 vegetation indices in 3 study sites was also subjected to an unsupervised classification
301 algorithm.

302 The ISODATA clustering algorithm was chosen due to its ability to split large diffuse clusters and to
303 merge small clusters whose centres are closer than a certain threshold (Memarsadeghi et al, 2007).
304 The ISODATA clustering routine processes data in an iterative manner, based on minimum Euclidean
305 distances between each pixel and the closest cluster in the multidimensional feature space of the
306 selected spectral bands. Throughout the clustering process, each iteration recalculates clusters' means
307 and reassigns pixels to the cluster with the closest mean value.

308 All study sites were clustered simultaneously to account for variations in light and atmospheric
309 conditions and the number of clusters was set to five, in agreement with the five plant communities
310 under study: Reed Swamp (RS), Lower Shore (LS), Upper Shore (US), Tall Grass (TG) and Open Pioneer
311 (OP). Prior to the clustering process, a Principal Component Analysis (PCA) was run on the input
312 variables. PCA has been widely use to extract uncorrelated variables from high dimensional
313 multispectral data (Zabalza et al, 2014). The variables or components extracted in a PCA convey most
314 of the spectral variability of the features under study and discard redundant information. Three
315 combinations of input data were tested in ISODATA: (1) PCA on individual spectral bands, (2) PCA on
316 the vegetation indices and (3) PCA on the vegetation indices and the spectral bands together. The first
317 three components were used in all cases as input variables. Analyses were performed in ArcGIS 10.3.

318

319 2.6 VALIDATION, CLASSIFICATION ACCURACY ASSESSMENT AND COMPARISONS BETWEEN MAPS

320 A Fleiss Kappa statistic was used to assess the overall mapping accuracy of the different classification
321 techniques (Ward et al., 2013). Based on the kappa statistic, the best performing algorithm was
322 selected for in-depth analysis. Although kappa statistics reveal clustering and classification

323 performances, additional tests are needed to explore in-depth classification accuracies for specific
324 plant communities. Community-specific classification accuracies may reveal differences in spectral
325 variability related to plant community composition and heterogeneity. An out-of-bag (OOB) estimate
326 of error was thus used to assess the prediction error of the RF algorithm for individual plant
327 communities (Gislason et al., 2006). In studies characterized by very high dimensionality, it is crucial to
328 estimate the importance of each predictive variable in classifying the data in order to determine the
329 variables performance. In order to detect the predictive power of the input variables within the RF
330 algorithm, the Mean Decrease in Accuracy (MDA) and Mean Decreased Gini (MDG) for individual
331 vegetation indices across all RF trees was analysed (Han et al., 2016). The Gini index is a measure of
332 the homogeneity and purity of nodes and leaves. Each time a variable is used to split a node in the RF
333 algorithm, the Gini index estimates the probability of a randomly chosen variable being wrongly
334 classified. By excluding one variable from the classification process, RF estimates the MDG. A higher
335 MDG indicates a higher variable importance in correctly splitting data in nodes across all trees
336 (Rodriguez-Galiano et al., 2012). RF also calculates the MDA by randomly permuting the values of a
337 certain variable in the OOB samples and subsequently recalculating the overall classification accuracy
338 of the model (Rodriguez-Galiano et al., 2012).

339 Beyond simple kappa-based comparisons, spatial comparisons between land cover maps have been
340 suggested as a tool to locate and quantify areas of land cover allocation disagreement (Gómez &
341 Montero, 2011). Detecting the spatial patterns of areas of disagreement may help identify
342 classification uncertainties associated with spectrally complex areas or transitional plant communities.
343 A spatial overlay was performed between the RF map and the map resulting from the best performing
344 ISODATA cluster. In addition, the statistics K_{location} (Pontius, 2000; Pontius, 2002) and K_{histo} (Hagen,
345 2002) were computed in order to provide an in-depth assessment of differences in the location and
346 the histogram shape of plant communities in all three locations. K_{histo} accounts for the
347 similarity/dissimilarity in the quantity of pixels belonging to the same category in two maps by
348 comparing the frequency of categories in both maps. When the frequency of categories in two maps
349 is equal, $K_{\text{histo}} = 1$. K_{location} compares the location of categories at the pixel level between two maps.
350 When two categories lie at identical locations, $K_{\text{location}} = 1$. The overall Kappa is computed as the product
351 of K_{location} and K_{histo} .

352 The kappa comparisons between the selected maps were performed in Map Comparison Kit (Visser
353 and De Nijs, 2006).

354

355 2.7 RELATIONSHIP BETWEEN SPECIES COMPOSITION, ABOVEGROUND BIOMASS AND SPECTRAL 356 SIGNATURE.

357 The methodology developed for this study characterizes within-sample spectral heterogeneity in
358 relation to species diversity and biomass in order to assess the impact on the classification accuracy of
359 the RF algorithm. In order to reduce the dimensionality of the spectral dataset, the spectral
360 heterogeneity was calculated as the standard deviation (SD) of the first principal component of the
361 individual bands. Species diversity was assessed using the Shannon index (H') for species abundance:

$$362 H' = -\sum_{i=1}^S p_i \ln(p_i)$$

363 Where

364 S = total number of species in the sampling plot

365 i = the i^{th} species

366 P = proportion of individuals of one particular species divided by the total number of individuals in the
367 sampling plot.

368 The Shannon index highlights the functional characteristics of the most abundant species (Rochinni et
369 al, 2010a) and is likely to be less affected by the presence of rare species than species richness. This
370 represents an adequate proxy for plant species composition in relation to spectral diversity.

371 A loess procedure (Cleveland et al., 1988) was applied to assess relationships between spectral
372 diversity and species diversity and aboveground biomass. Loess is a locally weighted regression model
373 that fits a function of the independent variable locally and in a moving fashion through a smoothing
374 process. The purpose of this analysis was to explore the spectral nature of training samples rather than
375 building a predictive model for species diversity and biomass. In this regard, loess offers a suitable
376 visualization procedure. Loess analysis was executed in R.

377

378 3. RESULTS

379 3.1 Comparison of classification models

380 The Fleiss' kappa classification accuracy for each method is shown in table 3 and the maps obtained
381 from different classification methods are shown in fig. 3. The overall classification accuracy was highest
382 for the Random Forest algorithm with 13 vegetation indices as input variables, with a Fleiss kappa
383 coefficient of 0.89. The PCA on the 13 vegetation indices plus the four individual bands improved the
384 classification accuracy of the unsupervised ISODATA algorithm from 0.31 (PCA on spectral bands) and
385 0.43 (PCA on vegetation indices) to 0.58.

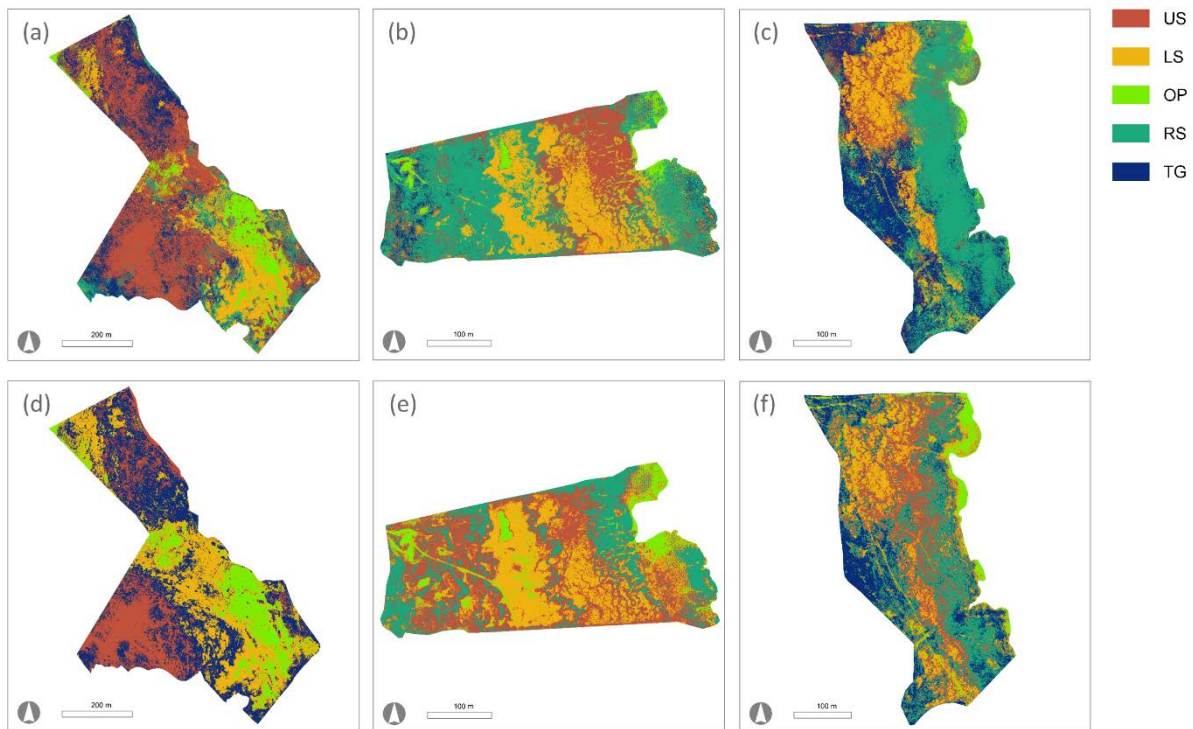
386 **Table 3:** Classification accuracy results for four different classification methods. A Fleiss' kappa
387 coefficient was used to determine the level of agreement between expected and observed plant
388 community types.

Classification method	Fleiss' kappa
Random Forest with vegetation indices	0.89
ISODATA clustering with PCA on spectral bands	0.31
ISODATA clustering with PCA on vegetation indices	0.43
ISODATA clustering with PCA on vegetation indices and spectral bands	0.58

389

390

391



392

393 **Fig. 3.** Classification results for Random Forest with vegetation indices in Kudani (a), Tahu N (b), Tahu
 394 S (c) and for ISODATA clustering with PCA on vegetation indices and spectral bands in Kudani (d), Tahu
 395 N (e) and Tahu S (f). US: Upper Shore, LS: Lower Shore, OP: Open Pioneer, RS: Reed Swamp, TG: Tall
 396 Grass.

397

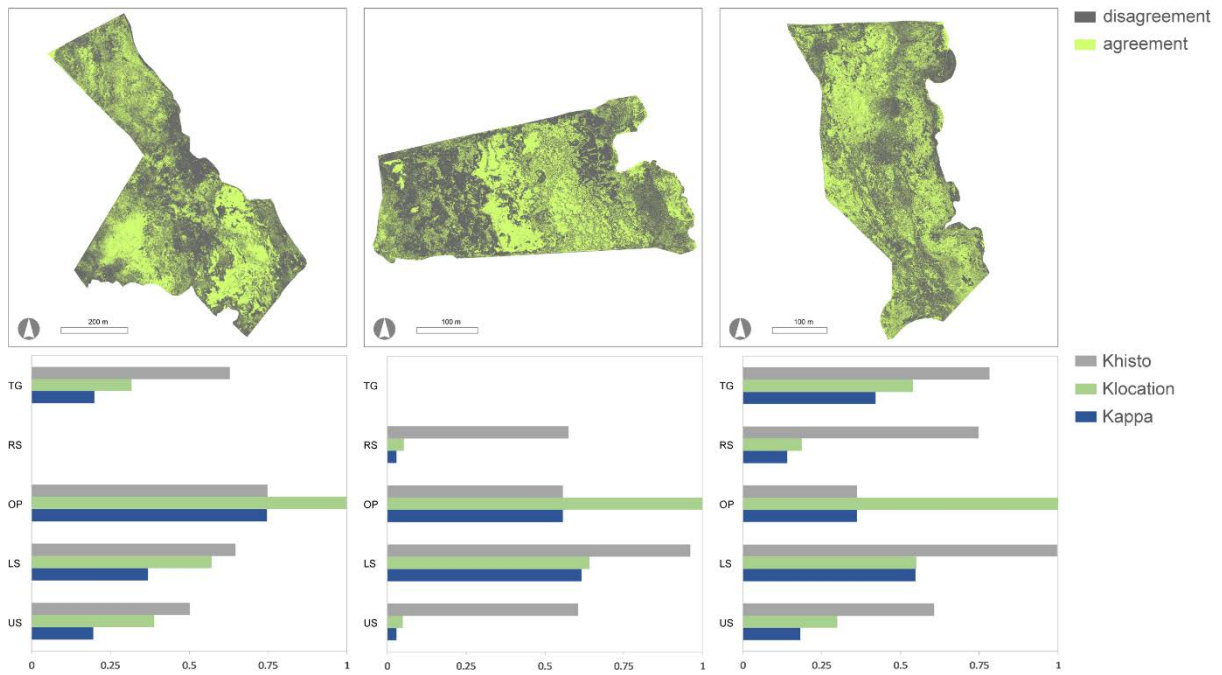
398 The comparison between the RF algorithm map and ISODATA clustering (PCA on vegetation indices
 399 and spectral bands) map yielded low levels of agreement (table 4). Tahu N shows the lowest values for
 400 overall Kappa (0.21) and $K_{location}$ (0.31), whereas Kudani shows the lowest levels of K_{histo} (0.57).

401 **Table 4.** Overall kappa, $K_{location}$ and K_{histo} results for the comparison between Random Forest and
 402 ISODATA maps. Kappa comparisons were performed individually for each study site.

Community	Kudani	Tahu N	Tahu S
Kappa	0.29	0.21	0.29
KLocation	0.51	0.31	0.39
KHisto	0.57	0.67	0.75

403

404 Fig. 4 provides a visual interpretation of areas of agreement and disagreement between both
 405 classifications and an overview of classification disagreements per community type. The highest levels
 406 of agreement reflected by overall kappa and $K_{location}$ and K_{histo} are reached in OP and LS respectively. RS
 407 and US show very low values of $K_{location}$ and moderate values of K_{histo} in Tahu N, indicating a certain
 408 degree of swapped classification between both communities, which can also be observed in fig 3.



409

410 **Fig 4.** Areas of classification disagreement between RF and ISODATA and overall Kappa, $K_{location}$ and K_{histo}
 411 values disaggregated per study site and community type.

412 **3.2 Random Forests accuracy assessment**

413 The performance of the RF classifier was further assessed with two statistical tests for classification
 414 accuracy. The out-of-bag (OOB) estimate of error highlighted the prediction error of RF for each plant
 415 community (table 5). The best classification accuracy corresponds to OP, with an OOB of 0.2%. RS and
 416 TG show the highest classification errors, with an OOB of and 13% and 18% respectively.

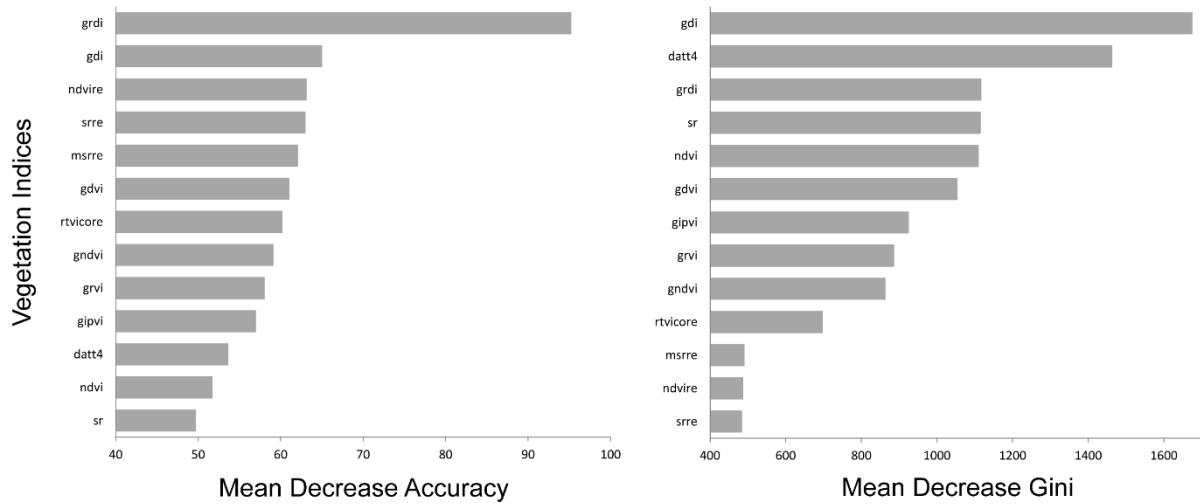
417 **Table 5.** OOB estimate of error of the RF classifier for each community type

Community	Class error
Reed Swamp (RS)	13%
Lower Shore (LS)	2%
Upper Shore (US)	10%
Open Pioneer (OP)	0.2%
Tall Grass (TG)	18%

418

419 The importance of the contribution of each predictor variable on the classification performance of RF
 420 was assessed by means of the Mean Decreased Accuracy (MDA) and Mean Decreased Gini (MDG) tests.
 421 According to the Gini index (fig. 5), the indices with the highest contribution to the RF model are GDI
 422 and DATT4, followed by GRDI and SR. The smallest contribution to the model's classification
 423 performance are SRRE, NDVIre and MSRRE. Regarding the Mean Decrease in Accuracy, the
 424 contribution of GRDI is the highest with a value of 95%. The contributions of GDI and NDVIre are also
 425 important with values of 65% and 63%. According to the MDA, NDVI and SR have the lowest
 426 importance, with values of 52% and 50% respectively.

427



428

429 **Fig. 5.** Mean Decreased Accuracy (MDA) and Mean Decreased Gini (MDG) values for all vegetation
 430 indices used as input variables in the RF classifier. Higher MDA and MDG values indicate a higher
 431 importance of the input variable in the classification process.

432 **3.3 PCA for spectral dimension reduction**

433 The best performing combination of input variables in the ISODATA algorithm was the three
 434 components of the PCA performed on the vegetation indices and spectral bands. The first three
 435 components explain 97% of the total variance in the multidimensional space (table 6). The first
 436 component is highly correlated with ratio-based vegetation indices incorporating the NIR band (NDVI,
 437 GNDVI and GIPVI) and a Red-Edge based index (DATT4). The second component is mainly correlated
 438 with the individual reflectance bands and two difference-based indices (GDVI and GDI). The third
 439 component relates to GRDI and SR.

440

441 **Table 6.** Eigenvectors of the vegetation indices and spectral bands and variance explained by each
 442 principal component

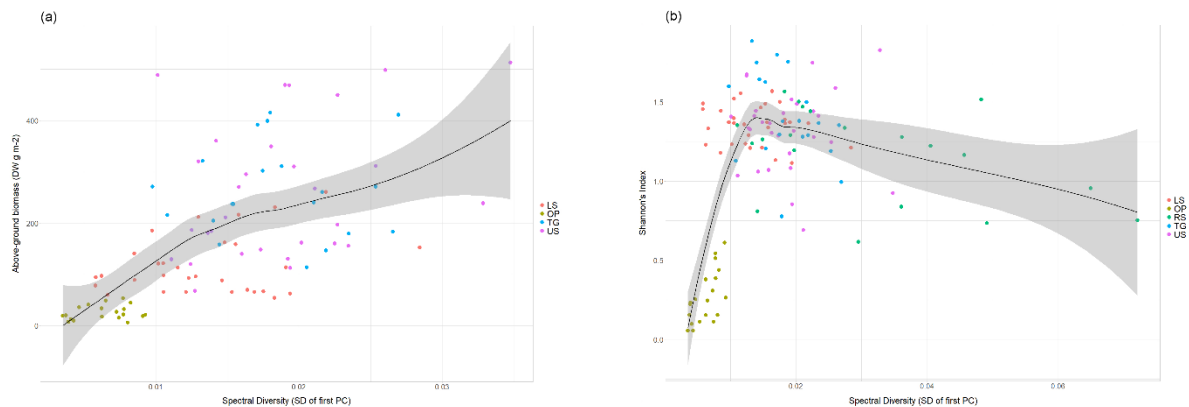
Vegetation indices/reflectance bands	1st component (82.4% variance explained)	2nd component (8.6% variance explained)	3rd component (5.9% variance explained)
NDVI	0.55		
GIPVI	0.46		
GNDVI	0.46		
DATT4	-0.22		
RED-EDGE		-0.48	
NIR		-0.43	
GDI		-0.42	
GDVI		-0.34	
GREEN		-0.26	
RED		-0.25	
GRDI			0.79
SR			0.24

443

444 **3.4 Relation between species composition, aboveground biomass and spectral signature**

445 A graphical comparison of the relationships between spectral diversity and species diversity and
446 biomass is provided in Fig. 6. Spectral diversity is more sensitive to biomass than to species diversity.
447 Although the relationship between spectral diversity and species diversity is initially positive, it
448 smoothly turns to negative after reaching the highest values of species diversity. It is worth noting that
449 all the plotted points around the negative section of the loess fitted curve (b) correspond to Reed
450 Swamp sampling plots.

451



452

453 **Fig. 6.** Relationships between aboveground biomass (a) and Shannon's index (b) vs. spectral diversity.
454 The fitted curves were obtained with a loess smoothing non-linear regression.

455

456 3. DISCUSSION

457 The rapid development of UAVs and lightweight sensors in recent years has widened the range of
458 remote sensing applications and solutions (Pajares, 2015). Simultaneously, an unprecedented volume
459 of very high spatial resolution remotely sensed data is being generated, posing a challenge in terms of
460 modelling and interpretation of results (Chi et al., 2016). While the availability of different modelling
461 techniques facilitates the processing of large amounts of remotely sensed data, it is still necessary to
462 understand the modelling capabilities and limitations in order to provide robust results. In this study,
463 a UAV was used to retrieve high-resolution multispectral images of three coastal meadows in West
464 Estonia. Subsequently, a RF model and an ISODATA algorithm were used to map plant communities at
465 the study sites.

466 The results show that the RF outperforms the ISODATA unsupervised classification algorithm (Table 3).
467 Specifically, the RF algorithm achieved very low per-class OOB errors for Open Pioneer and Lower
468 Shore (0.2% and 2% respectively) and increasingly higher for Upper Shore, Reed Swamp and Tall Grass
469 (10%, 13% and 18%). These differences in the classification error between communities can be
470 explained by the spectral characteristics of the vegetation and the training samples. The results of the
471 spectral signature analysis show that in the communities under study, species diversity is slightly
472 correlated with spectral diversity ($r = 0.23$) whereas aboveground biomass is moderately correlated
473 with spectral diversity ($r = 0.43$). This, in turn, has an effect on the characteristics of the training
474 samples and ultimately on the accuracy of the RF algorithm. For instance, low biomass communities
475 such as Lower Shore and communities with a very high proportion of bare ground such as Open Pioneer
476 present a very homogeneous spectral signature. Building upon homogeneous training samples, RF is
477 able to discriminate communities with a high level of precision. On the other hand, a higher
478 aboveground biomass and species diversity results in higher spectral diversity within the training

479 samples. This can be observed in the higher classification errors in Upper Shore (higher biomass and
480 diversity than Lower Shore and Open Pioneer), Reed Swamp (highest biomass) and Tall Grass (highest
481 diversity and high biomass).

482 Plant functional traits and morphological characteristics such as leaf size, branching structure, leaf
483 angle, etc. affect spectral reflectance (Schweiger et al., 2018). In this regard, the spectral diversity
484 hypothesis indicates that species within a community occupy spectral spaces defined by their
485 morphological characteristics (Rocchini et al., 2010a). Consequently, spectral diversity can be used as
486 a proxy for estimating the variability of plant traits within a certain area unit. Similarly, grassland
487 aboveground biomass may have an effect on the spectral variability of remotely sensed images,
488 especially at very high spatial resolutions. Recently grazed grassland patches may show a
489 homogeneous sward structure, especially in terms of sward height and biomass distribution. On the
490 other hand, swards undergoing a period of regrowth are commonly characterized by a complex
491 structure and a higher heterogeneity in both vertical and horizontal dimensions due to individual
492 plants differing in size, growth rates and biomass allocation (Marriott and Carrère, 1998, Wang et al.,
493 2018). Higher biomass swards are therefore expected to show a higher spectral variability. The
494 relationship between species diversity and spectral diversity has been previously studied in the context
495 of biodiversity monitoring, estimation and prediction (Rochinni et al., 2010) and has been tested across
496 a wide variety of habitats and spatial scales, including Mediterranean forests (Rocchini & Cade, 2008),
497 Amazonian tropical forests (Tuomisto et al., 2003) and African savannas (Rochinni et al., 2010b). In
498 contrast, while many studies focus on the use of multispectral imagery for biomass estimations
499 (Magiera et al., 2017; Punalekar et al., 2018; Naidoo et al., 2019), very few address the relationship
500 between biomass and spectral diversity. The results obtained in this study show that biomass and
501 species diversity have an influence on the characteristics and quality of the training samples. The loess
502 curve shown in Fig. 6a confirms the positive relationship between biomass and spectral diversity
503 described above. However, the relationship between species diversity and spectral diversity shown in
504 Fig. 6b suggests a more complex interaction. Increasing levels of species diversity correspond to
505 increased spectral diversity, as has been shown in previous studies. However, after reaching the
506 maximum level of species diversity, the curve turns negative indicating an increase in spectral diversity
507 as Shannon's diversity index decreases. This variation in the relationship can be attributed to two
508 phenomena. On one hand, the sensitivity of spectral diversity to biomass (Fig. 6a) could mask the effect
509 of species diversity. This is indicated by the fact that all the plotted points around the negative section
510 of the loess fitted curve in Fig. 6b correspond to Reed Swamp, which is characterized by a high biomass
511 and a relatively low level of species diversity. On the other hand, the very high spatial resolution
512 imagery provided by sensors mounted on UAVs may lead to artefacts. For instance, in communities
513 characterized by tall vegetation such as Reed Swamp, some pixels may fall in areas with direct sunlight
514 while others may fall in shaded areas or gaps between individual plants (Nagendra et al., 2010),
515 therefore increasing the spectral variability of the sample. These results highlight the need to account
516 for the nature and characteristics of spectral diversity when designing and adapting sampling strategies
517 for training plant community classification algorithms.

518 Regarding the variables importance in the classification accuracy of the RF algorithm, Green Red
519 Difference Index (GRDI) was shown to be the considerably more important than all other indices in
520 classifying plant communities according to the Mean Decreased Accuracy (MDA). The critical role of
521 GRDI in classifying grassland communities is likely to be related to its ability in predicting the
522 percentage of green herbage (Gianelle and Vescovo, 2007). GRDI has also been shown to be sensitive
523 to small changes in leaf colour and leaf density in grasslands (Motohka et al., 2010). Changes in green
524 reflectance captured by GRDI are likely to represent changes in pigment composition between plant
525 species in different communities.

526 Based on the classification purity metrics (Mean Decreased Gini), Green Difference Index (GDI) and
527 DATT4 were the most important predictor variables regarding increased data purity after each decision
528 tree node split. These results indicate that GDI and DATT4 show a superior performance to other
529 vegetation indices in terms of obtaining pure classes at the end of the classification process. Similarly
530 to GRDI, GDI may capture changes in green reflectance better than some other indices (e.g. NDVI).
531 DATT4 is a red-edge-based index proposed by Datt (1998) as an alternative to NDVI and GNDVI to
532 maximize the sensitivity to changes in pigment concentration in leaves. A sharp change of reflectance
533 occurs in the red-edge region, related to the transition from chlorophyll absorption to leaf scattering
534 (Delegido et al., 2013). Consequently, the red-edge band has been proven to be very sensitive to
535 variations in chlorophyll *a*, *b* and carotenoids (Adamczyk, 2015) and therefore its use in vegetation
536 indices reduces the saturation effect known to affect e.g. NDVI (Clevers and Gitelson, 2013). This
537 explains the key role of DATT4 in the correct classification of plant communities in coastal meadows.

538 On the other hand, NDVI shows a very low contribution to MDA, which highlights its marginal role in
539 the overall performance of the model. Previous studies suggest NDVI is a poor indicator of forest
540 phenology due to its low sensitivity to leaf colour change (Motohka et al., 2010). In addition, using
541 NDVI can present some limitations due to its sensitivity to the effects of soil brightness, soil colour,
542 atmosphere and leaf canopy shadow (Xue & Su, 2017) and shows saturation in high density vegetation
543 (Gu et al., 2013). NDVI is therefore likely to also exhibit a low sensitivity to different rates of leaf
544 senescence and proportions of chlorophyll and other pigments in grasslands.

545 Within this study, an unsupervised classification method was tested in order to compare its
546 performance with the RF algorithm. The ISODATA clustering algorithm reduces costs associated with
547 the training sample collection process. However, the classification accuracy obtained with the different
548 combinations of input variables in ISODATA was considerably lower than RF. The best results were
549 obtained by combining all vegetation indices and individual spectral bands in a PCA (Table 3) and
550 subsequently using the first three components as input variables in the ISODATA clustering algorithm.
551 Mixing individual spectral bands with vegetation indices in the PCA generated a component entirely
552 correlated with the spectral bands (PC2). On the other hand, PC1 incorporated three NIR ratio-based
553 vegetation indices (NDVI, GNDVI and GIPVI) and a Red-Edge based index (DATT4). The highest
554 contribution to PC2 is the red-edge band, which highlights the key role of this band in discerning
555 vegetation types. The clear separation between indices and bands in different components is likely due
556 to the fact that non-normalized spectral bands tend to be correlated among themselves. In fact, the
557 only vegetation indices included in PC2 are non-normalized and also likely correlated with the spectral
558 bands. In previous studies, PCA has been used to compute synthetic bands that are subsequently
559 utilized as input variables in supervised classification algorithms (Yesilnacar & Süzen, 2006; Novelli et
560 al., 2016) with high classification accuracies. The results in this study highlight that the classes obtained
561 in unsupervised classification do not necessarily correspond to different plant communities on the
562 ground. Nevertheless, these methods provide a good overview of spectral differences over the whole
563 dataset.

564 Fleiss kappa comparisons between plant community classification techniques offer a quick and simple
565 way to assess classification accuracy (Landis & Koch, 1977; Chmura Kraemer, 1980). However, Fleiss
566 kappa fails to provide information on the spatial nature of the agreement and disagreement between
567 classification techniques (Gómez & Montero, 2011). This information is essential, as it helps identify
568 communities characterized by very high spectral heterogeneity due to factors such as disturbance or
569 communities located within or adjacent to ecotones. An assessment of classification disagreement was
570 performed by overlying the RF map with the ISODATA (PCA on bands plus indices) map. The results
571 show that at the study sites, some areas of disagreement correspond to disturbed communities such

572 as a recently restored patch of grassland in the western section of Tahu N or certain sections in Kudani
573 over-trampled by cattle. Similarly, transition areas between Reed Swamp, Tall Grass and Upper Shore
574 show disagreement in the three study sites, perhaps due to structural differences in these ecotones.
575 In addition to the visual interpretation, a kappa map comparison analysis was performed in order to
576 gain a deeper understanding of the characteristics of disagreement between classifications. Generally,
577 the most productive communities (Reed Swamp, Tall Grass and Upper Shore) show the lowest degree
578 of agreement in all three sites, with very low values of $K_{location}$, especially at Tahu N. Although values of
579 K_{histo} are moderate for these communities, low $K_{location}$ indicates incorrectly predicted community
580 locations from the ISODATA algorithm. This is most likely due to the presence of large sections of
581 disturbed and transitional communities and the spectral heterogeneity of communities characterized
582 by higher biomass production such as Tall Grass and Reed Swamp.

583 This study demonstrates the feasibility of using vegetation indices derived from UAV imagery for the
584 classification of plant communities in coastal meadows. The RF model accurately predicted the
585 occurrence of plant communities with a very high kappa value. Previous studies have used similar
586 approaches to discern and map spectrally distant land cover classes such as forest and meadows (Feng
587 et al., 2015; Ahmed et al., 2017) or distinguish crop types (Lottes et al., 2017; Böhler et al., 2018).
588 However, few studies have attempted to map spectrally similar landscape patches at the plant
589 community scale (Strong et al., 2017, Rapinel et al., 2019). The results obtained in this study highlight
590 the need to consider a wide range of vegetation indices in order to achieve the best differentiation
591 between plant communities. Moreover, few studies have attempted to assess the spectral nature of
592 training samples in relation to community structure and composition (Goodwin et al., 2005). Beyond
593 the number of training samples, training polygon size and image resolution, the spectral heterogeneity
594 within the training samples has an impact on the accuracy of the classifications obtained from
595 supervised algorithms. Training datasets with a higher spectral diversity may reduce the ability of
596 machine learning algorithms to discriminate between different plant communities. This study
597 demonstrates the need to assess the spectral characteristics of training samples in order to gain a full
598 understanding of the performance of classification algorithms.

599

600 5. CONCLUSIONS

601

602 Multispectral UAV imagery was successfully used to classify five plant community types in high
603 biodiversity value coastal meadows in West Estonia. The results demonstrate that an appropriate
604 sampling strategy and choice of vegetation indices yield accurate plant community maps. While UAV
605 multispectral imagery in combination with classification algorithms constitute a valuable tool in habitat
606 management and nature conservation contexts, there are several important areas that require
607 attention. Species diversity and biomass heavily influence the spectral characteristics and quality of
608 training samples at different plant communities. This should be accounted for in the design phase of
609 the sample collection process in order to achieve the best classification accuracies. Moreover, it is
610 crucial to utilize a wide array of vegetation indices in order to avoid poor results associated with less
611 sensitive indices such as NDVI. In this regard, the use of the red-edge band delivers good results due
612 to its sensitivity to chlorophylls, carotenoids and other pigments. This study has provided a novel
613 method for mapping grasslands at a plant community level using plant species and biomass data
614 together with random forest modelling utilising a range of different vegetation indices. Future research
615 should further address the optimization of training sample acquisition, modelling algorithms and
616 sample spectral characteristics.

617

618 Acknowledgements

619 This work was supported by institutional research funding IUT21-1 at the Estonian Ministry of
620 Education and Research.

621 5. REFERENCES

622

- 623 1. Aasen, H., Burkart, A., Bolten, A., & Bareth, G. (2015). Generating 3D hyperspectral
624 information with lightweight UAV snapshot cameras for vegetation monitoring: From camera
625 calibration to quality assurance. *ISPRS Journal of Photogrammetry and Remote Sensing*, *108*,
626 245-259. doi:10.1016/j.isprsjprs.2015.08.002
- 627 2. Adamczyk, J., & Osberger, A. (2015). Red-edge vegetation indices for detecting and assessing
628 disturbances in Norway spruce dominated mountain forests. *International Journal of Applied*
629 *Earth Observation and Geoinformation*, *37*, 90-99. doi:10.1016/j.jag.2014.10.013
- 630 3. Adão, T., Hruška, J., Pádua, L., Bessa, J., Peres, E., Morais, R., & Sousa, J. (2017).
631 Hyperspectral Imaging: A Review on UAV-Based Sensors, Data Processing and Applications
632 for Agriculture and Forestry. *Remote Sensing*, *9*(11), 1110. doi:10.3390/rs9111110
- 633 4. Ahmed, O. S., Shemrock, A., Chabot, D., Dillon, C., Williams, G., Wasson, R., & Franklin, S. E.
634 (2017). Hierarchical land cover and vegetation classification using multispectral data acquired
635 from an unmanned aerial vehicle. *International Journal of Remote Sensing*, *38*(8-10), 2037-
636 2052. doi:10.1080/01431161.2017.1294781
- 637 5. Armitage, A. R., Highfield, W. E., Brody, S. D., & Louchouart, P. (2015). The Contribution of
638 Mangrove Expansion to Salt Marsh Loss on the Texas Gulf Coast. *Plos One*, *10*(5).
639 doi:10.1371/journal.pone.0125404
- 640 6. Baena, S., Boyd, D. S., & Moat, J. (2018). UAVs in pursuit of plant conservation - Real world
641 experiences. *Ecological Informatics*, *47*, 2-9. doi:10.1016/j.ecoinf.2017.11.001
- 642 7. Balzarolo, M., Arriga, N., & Papale, D. (2009, April). LAI estimation in a Mediterranean
643 grassland by in situ radiometric measurements and MODIS satellite data. In *EGU General*
644 *Assembly Conference Abstracts* (Vol. 11, p. 9216).
- 645 8. Belgiu, M., & Drăguț, L. (2016). Random forest in remote sensing: A review of applications
646 and future directions. *ISPRS Journal of Photogrammetry and Remote Sensing*, *114*, 24-31.
647 doi:10.1016/j.isprsjprs.2016.01.011
- 648 9. Benkert, D. (2008). Ellenberg, Heinz, Zeigerwerte der Gefäßpflanzen Mitteleuropas. 2. Aufl.
649 Scripta Geobotanica IX. 122 S. Erich Goltze KG. Göttingen, 1979. Kartoniert, DM 21. *Feddes*
650 *Repertorium*, *91*(4), 268-269. doi:10.1002/fedr.19800910408
- 651 10. Berg, M., Joyce, C., & Burnside, N. (2011). Differential responses of abandoned wet grassland
652 plant communities to reinstated cutting management. *Hydrobiologia*, *692*(1), 83-97.
653 doi:10.1007/s10750-011-0826-x
- 654 11. Berni, J., Zarco-Tejada, P., Suarez, L., & Fereres, E. (2009). Thermal and Narrowband
655 Multispectral Remote Sensing for Vegetation Monitoring From an Unmanned Aerial
656 Vehicle. *IEEE Transactions on Geoscience and Remote Sensing*, *47*(3), 722-738.
657 doi:10.1109/tgrs.2008.2010457
- 658 12. Bivand, R., Keitt, T., Rowlingson, B., Pebesma, E., Sumner, M., Hijmans, R., ... & Bivand, M. R.
659 (2015). Package 'rgdal'. Bindings for the Geospatial Data Abstraction Library. Available
660 online: <https://cran.r-project.org/web/packages/rgdal/index.html> (accessed on 15 October
661 2017).
- 662 13. Blaschke, T. (2010). Object based image analysis for remote sensing. *ISPRS Journal of*
663 *Photogrammetry and Remote Sensing*, *65*(1), 2–16. doi: 10.1016/j.isprsjprs.2009.06.004
- 664 14. Breiman, L. (2001). Random forests. *Machine learning*, *45*(1), 5-32. doi:
665 10.1023/A:1010933404324

- 666 15. Brotherton, S. J., & Joyce, C. B. (2014). Extreme climate events and wet grasslands: Plant
667 traits for ecological resilience. *Hydrobiologia*, 750(1), 229-243. doi:10.1007/s10750-014-2129-
668 5
- 669 16. Brown, M., Pinzon, J., Didan, K., Morisette, J., & Tucker, C. (2006). Evaluation of the
670 consistency of long-term NDVI time series derived from AVHRR, SPOT-vegetation, SeaWiFS,
671 MODIS, and Landsat ETM sensors. *IEEE Transactions on Geoscience and Remote*
672 *Sensing*, 44(7), 1787-1793. doi:10.1109/tgrs.2005.860205
- 673 17. Burkhard, B., & Maes, J. (2017). Mapping ecosystem services. Advanced Books, 1, e12837
- 674 18. Burnside, N. G., Joyce, C. B., Puurmann, E., & Scott, D. M. (2007). Use of vegetation
675 classification and plant indicators to assess grazing abandonment in Estonian coastal
676 wetlands. *Journal of Vegetation Science*, 18(5), 645. doi:10.1658/1100-
677 9233(2007)18[645:uovcap]2.0.co;2
- 678 19. Burnside, N. and Waite, S. (2011) Predictive modelling of biogeographical phenomena. In:
679 Millington, A., Blumler, M. and Schikhoff, U. The SAGE handbook of biogeography. SAGE
680 Publications Ltd. UK.
- 681 20. Böhler, J., Schaepman, M., & Kneubühler, M. (2018). Crop Classification in a Heterogeneous
682 Arable Landscape Using Uncalibrated UAV Data. *Remote Sensing*, 10(8), 1282.
683 doi:10.3390/rs10081282
- 684 21. Candiago, S., Remondino, F., Giglio, M. D., Dubbini, M., & Gattelli, M. (2015). Evaluating
685 Multispectral Images and Vegetation Indices for Precision Farming Applications from UAV
686 Images. *Remote Sensing*, 7(4), 4026-4047. doi:10.3390/rs70404026
- 687 22. Cardinale, B. J., Duffy, J. E., Gonzalez, A., Hooper, D. U., Perrings, C., Venail, P., . . . Naeem, S.
688 (2012). Biodiversity loss and its impact on humanity. *Nature*, 486(7401), 59-67.
689 doi:10.1038/nature11148
- 690 23. Cavender-Bares, J., Gamon, J. A., Hobbie, S. E., Madritch, M. D., Meireles, J. E., Schweiger, A.
691 K., & Townsend, P. A. (2017). Harnessing plant spectra to integrate the biodiversity sciences
692 across biological and spatial scales. *American Journal of Botany*, 104(7), 966-969.
693 doi:10.3732/ajb.1700061
- 694 24. Chen, D., & Stow, D. (2002). The effect of training strategies on supervised classification at
695 different spatial resolutions. *Photogrammetric Engineering and Remote Sensing*, 68(11),
696 1155-1162.
- 697 25. Chi, M., Plaza, A., Benediktsson, J. A., Sun, Z., Shen, J., & Zhu, Y. (2016). Big Data for Remote
698 Sensing: Challenges and Opportunities. *Proceedings of the IEEE*, 104(11), 2207-2219.
699 doi:10.1109/jproc.2016.2598228
- 700 26. Chmura Kraemer, H. (1980). Extension of the Kappa Coefficient. *Biometrics*, 36(2), 207.
701 doi:10.2307/2529972
- 702 27. Clausen, K. K., Stjernholm, M., & Clausen, P. (2013). Grazing management can counteract the
703 impacts of climate change-induced sea level rise on salt marsh-dependent
704 waterbirds. *Journal of Applied Ecology*, 50(2), 528-537. doi:10.1111/1365-2664.12043
- 705 28. Cleveland, W. S., & Devlin, S. J. (1988). Locally weighted regression: an approach to
706 regression analysis by local fitting. *Journal of the American statistical association*, 83(403),
707 596-610.
- 708 29. Clevers, J., & Gitelson, A. (2013). Remote estimation of crop and grass chlorophyll and
709 nitrogen content using red-edge bands on Sentinel-2 and -3. *International Journal of Applied*
710 *Earth Observation and Geoinformation*, 23, 344-351. doi:10.1016/j.jag.2012.10.008
- 711 30. Cook, K. L. (2017). An evaluation of the effectiveness of low-cost UAVs and structure from
712 motion for geomorphic change detection. *Geomorphology*, 278, 195-208.
713 doi:10.1016/j.geomorph.2016.11.009
- 714 31. Crawley, M. J. (Ed.). (1997) Plant ecology. *Blackwell Publishing*
715 Ltd. <http://dx.doi.org/10.1002/9781444313642>
- 716 32. Crippen, R. (1990). Calculating the vegetation index faster. *Remote Sensing of*
717 *Environment*, 34(1), 71-73. doi:10.1016/0034-4257(90)90085-z

- 718 33. Crossman, N. D., Burkhard, B., Nedkov, S., Willemsen, L., Petz, K., Palomo, I., . . . Maes, J.
719 (2013). A blueprint for mapping and modelling ecosystem services. *Ecosystem Services*, 4, 4-
720 14. doi:10.1016/j.ecoser.2013.02.001
- 721 34. Datt, B. (1998). Remote Sensing of Chlorophyll a, Chlorophyll b, Chlorophyll a b, and Total
722 Carotenoid Content in Eucalyptus Leaves. *Remote Sensing of Environment*, 66(2), 111-121.
723 doi:10.1016/S0034-4257(98)00046-7
- 724 35. Davidson, S., Santos, M., Sloan, V., Watts, J., Phoenix, G., Oechel, W., & Zona, D. (2016).
725 Mapping Arctic Tundra Vegetation Communities Using Field Spectroscopy and Multispectral
726 Satellite Data in North Alaska, USA. *Remote Sensing*, 8(12), 978. doi:10.3390/rs8120978
- 727 36. Delegido, J., Verrelst, J., Meza, C., Rivera, J., Alonso, L., & Moreno, J. (2013). A red-edge
728 spectral index for remote sensing estimation of green LAI over agroecosystems. *European*
729 *Journal of Agronomy*, 46, 42-52. doi:10.1016/j.eja.2012.12.001
- 730 37. Diekmann, M. (2003). Species indicator values as an important tool in applied plant ecology –
731 a review. *Basic and Applied Ecology*, 4(6), 493-506. doi:10.1078/1439-1791-00185
- 732 38. Dietterich, T. G. (2000). An experimental comparison of three methods for constructing
733 ensembles of decision trees: Bagging, boosting, and randomization. *Machine learning*, 40(2),
734 139-157. doi: 10.1023/A:1007607513941
- 735 39. Dimitriadou, E., Hornik, K., Leisch, F., Meyer, D., Weingessel, A., & Leisch, M. F. (2006). The
736 e1071 package. Misc Functions of Department of Statistics (e1071), TU Wien.
- 737 40. Duda, T., & Canty, M. (2002). Unsupervised classification of satellite imagery: Choosing a
738 good algorithm. *International Journal of Remote Sensing*, 23(11), 2193-2212.
739 doi:10.1080/01431160110078467
- 740 41. EFN and RDSNC. (2001). The inventory of semi-natural grasslands in Estonia 1999-2001: Final
741 report. *Estonian Fund for Nature and Royal Dutch Society for Nature Conservation*, Estonia.
- 742 42. Ellenberg, H. (1979) Zeigerwerte der Gefasspflanzen Mitteleuropas. *Scripta Geobotanica* 9:
743 42-111.
- 744 43. Everitt, J. H., Yang, C., & Deloach, C. J. (2005). Remote sensing of giant reed with QuickBird
745 satellite imagery. *Journal of Aquatic Plant Management*, 43, 81-85.
- 746 44. Feng, Q., Liu, J., & Gong, J. (2015). UAV Remote Sensing for Urban Vegetation Mapping Using
747 Random Forest and Texture Analysis. *Remote Sensing*, 7(1), 1074-1094.
748 doi:10.3390/rs70101074
- 749 45. Forsmo, J., Anderson, K., Macleod, C. J., Wilkinson, M. E., & Brazier, R. (2018). Drone-based
750 structure-from-motion photogrammetry captures grassland sward height variability. *Journal*
751 *of Applied Ecology*, 55(6), 2587-2599. doi:10.1111/1365-2664.13148
- 752 46. Gianelle, D., & Vescovo, L. (2007). Determination of green herbage ratio in grasslands using
753 spectral reflectance. Methods and ground measurements. *International Journal of Remote*
754 *Sensing*, 28(5), 931-942. doi:10.1080/01431160500196398
- 755 47. Gislason, P. O., Benediktsson, J. A., & Sveinsson, J. R. (2006). Random Forests for land cover
756 classification. *Pattern Recognition Letters*, 27(4), 294-300. doi:10.1016/j.patrec.2005.08.011
- 757 48. Gitelson, A. A., Kaufman, Y. J., & Merzlyak, M. N. (1996). Use of a green channel in remote
758 sensing of global vegetation from EOS-MODIS. *Remote Sensing of Environment*, 58(3), 289-
759 298. doi:10.1016/S0034-4257(96)00072-7
- 760 49. Gitelson, A., & Merzlyak, M. N. (1994). Spectral Reflectance Changes Associated with Autumn
761 Senescence of *Aesculus hippocastanum* L. and *Acer platanoides* L. Leaves. Spectral Features
762 and Relation to Chlorophyll Estimation. *Journal of Plant Physiology*, 143(3), 286-292.
763 doi:10.1016/S0176-1617(11)81633-0
- 764 50. Gomez, D., & Montero, J. (2011). Determining the accuracy in image supervised classification
765 problems. *Proceedings of the 7th Conference of the European Society for Fuzzy Logic and*
766 *Technology (EUSFLAT-2011)*. doi:10.2991/eusflat.2011.103
- 767 51. Gonçalves, J., Henriques, R., Alves, P., Sousa-Silva, R., Monteiro, A. T., Lomba, Â, . . . Honrado,
768 J. (2015). Evaluating an unmanned aerial vehicle-based approach for assessing habitat extent

- 769 and condition in fine-scale early successional mountain mosaics. *Applied Vegetation*
770 *Science*,19(1), 132-146. doi:10.1111/avsc.12204
- 771 52. Goodwin, N., Turner, R., & Merton, R. (2005). Classifying Eucalyptus forests with high spatial
772 and spectral resolution imagery: An investigation of individual species and vegetation
773 communities. *Australian Journal of Botany*, 53(4), 337. doi:10.1071/bt04085
- 774 53. Gu, Y., Wylie, B. K., Howard, D. M., Phuyal, K. P., & Ji, L. (2013). NDVI saturation adjustment:
775 A new approach for improving cropland performance estimates in the Greater Platte River
776 Basin, USA. *Ecological Indicators*,30, 1-6. doi:10.1016/j.ecolind.2013.01.041
- 777 54. Hagen, A. (2002, April). Multi-method assessment of map similarity. In Proceedings of the 5th
778 AGILE Conference on Geographic Information Science (pp. 171-182). Palma, Spain:
779 Universitat de les Illes Balears
- 780 55. Hamada, Y., Stow, D. A., & Roberts, D. A. (2011). Estimating life-form cover fractions in
781 California sage scrub communities using multispectral remote sensing. *Remote Sensing of*
782 *Environment*,115(12), 3056-3068. doi:10.1016/j.rse.2011.06.008
- 783 56. Han, H., Guo, X., & Yu, H. (2016). Variable selection using Mean Decrease Accuracy and Mean
784 Decrease Gini based on Random Forest. *2016 7th IEEE International Conference on Software*
785 *Engineering and Service Science (ICSESS)*. doi:10.1109/icsess.2016.7883053
- 786 57. Henle, K., Alard, D., Clitherow, J., Cobb, P., Firbank, L., Kull, T., . . . Young, J. (2008). Identifying
787 and managing the conflicts between agriculture and biodiversity conservation in Europe—A
788 review. *Agriculture, Ecosystems & Environment*,124(1-2), 60-71.
789 doi:10.1016/j.agee.2007.09.005
- 790 58. Hijmans, R. J. & van Etten, J. (2012). raster: Geographic analysis and modeling with raster
791 data. R package version 2.0-12. <http://CRAN.R-project.org/package=raster>
- 792 59. Houborg, R., & McCabe, M. (2016). High-Resolution NDVI from Planet's Constellation of Earth
793 Observing Nano-Satellites: A New Data Source for Precision Agriculture. *Remote Sensing*,8(9),
794 768. doi:10.3390/rs8090768
- 795 60. Ingerpuu, N., & Sarv, M. (2015). Effect of Grazing on Plant Diversity of Coastal Meadows in
796 Estonia. *Annales Botanici Fennici*,52(1-2), 84-92. doi:10.5735/085.052.0210
- 797 61. IPCC. (2013). Climate change 2013: Synthesis Report. *Cambridge University Press*, UK.
- 798 62. Jensen, J. R. (2007). *Remote sensing of the environment: An earth resource perspective*.
799 Upper Saddle River, NJ: Prentice-Hall International.
- 800 63. Jones, H. G., & Vaughan, R. A. (2010). *Remote sensing of vegetation: principles, techniques,*
801 *and applications*. Oxford university press..
- 802 64. Jordan, C. F. (1969). Derivation of Leaf-Area Index from Quality of Light on the Forest
803 Floor. *Ecology*,50(4), 663-666. doi:10.2307/1936256
- 804 65. Joyce, C. B. (2014). Ecological consequences and restoration potential of abandoned wet
805 grasslands. *Ecological Engineering*,66, 91-102. doi:10.1016/j.ecoleng.2013.05.008
- 806 66. Joyce, C. B., Simpson, M., & Casanova, M. (2016). Future wet grasslands: Ecological
807 implications of climate change. *Ecosystem Health and Sustainability*,2(9).
808 doi:10.1002/ehs2.1240
- 809 67. Jones, H. & Vaughan, R. (2010) Remote Sensing of Vegetation Principle Techniques and
810 Applications. *Oxford University Press*, UK.
- 811 68. Keskkonnaamet (2017) Silma looduskaitseala ja Karjatsimere hoivuala kaitsekorralduskava
812 2017–2026
- 813 69. Kuhn, M. (2012). The caret package. R Foundation for Statistical Computing, Vienna, Austria.
814 URL [https://cran.r-project.org/package= caret](https://cran.r-project.org/package=caret).
- 815 70. Landis, J. R., & Koch, G. G. (1977). The Measurement of Observer Agreement for Categorical
816 Data. *Biometrics*, 33(1), 159. doi:10.2307/2529310
- 817 71. Leito, A., Elts, J., Mägi, E., Ivask, I., Ööpik, M., Sepp, K. & Ward, R.D. (2014) Coastal grassland
818 wader abundance in relation to breeding habitat characteristics and prey abundance in
819 Matsalu, Estonia. *Ornis Fennica* 91, 149-165.

- 820 72. Liaw, A. & Wiener, M. (2002). Classification and Regression by randomForest. *R News* 2(3),
821 18--22.
- 822 73. Liu, D., & Xia, F. (2010). Assessing object-based classification: advantages and limitations.
823 *Remote Sensing Letters*, 1(4), 187-194.
- 824 74. Lottes, P., Khanna, R., Pfeifer, J., Siegwart, R., & Stachniss, C. (2017). UAV-based crop and
825 weed classification for smart farming. *2017 IEEE International Conference on Robotics and*
826 *Automation (ICRA)*. doi:10.1109/icra.2017.7989347
- 827 75. Lu, B., & He, Y. (2017). Species classification using Unmanned Aerial Vehicle (UAV)-acquired
828 high spatial resolution imagery in a heterogeneous grassland. *ISPRS Journal of*
829 *Photogrammetry and Remote Sensing*, 128, 73-85. doi:10.1016/j.isprsjprs.2017.03.011
- 830 76. Mafi-Gholami, D., Zenner, E. K., Jaafari, A., & Ward, R. D. (2019). Modeling multi-decadal
831 mangrove leaf area index in response to drought along the semi-arid southern coasts of Iran.
832 *Science of The Total Environment*, 656, 1326-1336. doi:10.1016/j.scitotenv.2018.11.462
- 833 77. Marriott, C. A., & Carrère, P. (1998). Structure and dynamics of grazed vegetation. *Annales*
834 *De Zootechnie*, 47(5-6), 359-369. doi:10.1051/animres:19980504
- 835 78. Medina, O., Manian, V., & Chinea, J. (2013). Biodiversity Assessment Using Hierarchical
836 Agglomerative Clustering and Spectral Unmixing over Hyperspectral Images. *Sensors*, 13(10),
837 13949-13959. doi:10.3390/s131013949
- 838 79. Memarsadeghi, N., Mount, D. M., Netanyahu, N. S., & Moigne, J. L. (2007). A Fast
839 Implementation Of The Isodata Clustering Algorithm. *International Journal of Computational*
840 *Geometry & Applications*, 17(01), 71-103. doi:10.1142/s0218195907002252
- 841 80. Motohka, T., Nasahara, K. N., Oguma, H., & Tsuchida, S. (2010). Applicability of Green-Red
842 Vegetation Index for Remote Sensing of Vegetation Phenology. *Remote Sensing*, 2(10), 2369-
843 2387. doi:10.3390/rs2102369
- 844 81. Mueller-Dombois, D., & Ellenberg, H. (1974). Aims and methods of vegetation ecology. *Wiley*
- 845 82. Nagendra, H., Rocchini, D., Ghate, R., Sharma, B., & Pareeth, S. (2010). Assessing Plant
846 Diversity in a Dry Tropical Forest: Comparing the Utility of Landsat and Ikonos Satellite
847 Images. *Remote Sensing*, 2(2), 478-496. doi: 10.3390/rs2020478
- 848 83. Naidoo, L., Deventer, H. V., Ramoelo, A., Mathieu, R., Nondlazi, B., & Gangat, R. (2019).
849 Estimating above ground biomass as an indicator of carbon storage in vegetated wetlands of
850 the grassland biome of South Africa. *International Journal of Applied Earth Observation and*
851 *Geoinformation*, 78, 118-129. doi:10.1016/j.jag.2019.01.021
- 852 84. Navarro, G., Caballero, I., Silva, G., Parra, P., Vázquez, Á, & Caldeira, R. (2017). Evaluation of
853 forest fire on Madeira Island using Sentinel-2A MSI imagery. *International Journal of Applied*
854 *Earth Observation and Geoinformation*, 58, 97-106. doi:10.1016/j.jag.2017.02.003
- 855 85. Newbold, T., Hudson, L. N., Arnell, A. P., Contu, S., Palma, A. D., Ferrier, S., . . . Purvis, A.
856 (2016). Has land use pushed terrestrial biodiversity beyond the planetary boundary? A global
857 assessment. *Science*, 353(6296), 288-291. doi:10.1126/science.aaf2201
- 858 86. Novelli, A., Tarantino, E., Caradonna, G., Apollonio, C., Balacco, G., & Piccinni, F. (2016).
859 Improving the ANN Classification Accuracy of Landsat Data Through Spectral Indices and
860 Linear Transformations (PCA and TCT) Aimed at LU/LC Monitoring of a River Basin.
861 *Computational Science and Its Applications – ICCSA 2016 Lecture Notes in Computer Science*,
862 420-432. doi:10.1007/978-3-319-42108-7_32
- 863 87. Oldeland, J., Wesuls, D., Rocchini, D., Schmidt, M., & Jürgens, N. (2010). Does using species
864 abundance data improve estimates of species diversity from remotely sensed spectral
865 heterogeneity? *Ecological Indicators*, 10(2), 390-396. doi:10.1016/j.ecolind.2009.07.012
- 866 88. Paal, J. (1998). Rare and threatened plant communities of Estonia. *Biodiversity &*
867 *Conservation*, 7(8), 1027-1049. Pajares, G. (2015). Overview and Current Status of Remote
868 Sensing Applications Based on Unmanned Aerial Vehicles (UAVs). *Photogrammetric*
869 *Engineering & Remote Sensing*, 81(4), 281-330. doi:10.14358/pers.81.4.281

- 870 89. Pajares, G. (2015). Overview and Current Status of Remote Sensing Applications Based on
871 Unmanned Aerial Vehicles (UAVs). *Photogrammetric Engineering & Remote Sensing*, 81(4),
872 281-330. doi:10.14358/pers.81.4.281
- 873 90. Pontius, R. G. (2001). Quantification error versus location error in comparison of categorical
874 maps (vol 66, pg 1011, 2000). *Photogrammetric Engineering and Remote Sensing*, 67(5), 540-
875 540
- 876 91. Pontius, R. G. (2002). Statistical methods to partition effects of quantity and location during
877 comparison of categorical maps at multiple resolutions. *Photogrammetric Engineering and*
878 *Remote Sensing*, 68(10), 1041-1050.
- 879 92. Punalekar, S., Verhoef, A., Quaife, T., Humphries, D., Bermingham, L., & Reynolds, C. (2018).
880 Application of Sentinel-2A data for pasture biomass monitoring using a physically based
881 radiative transfer model. *Remote Sensing of Environment*, 218, 207-220.
882 doi:10.1016/j.rse.2018.09.028
- 883 93. Punalekar, S., Verhoef, A., Quaife, T., Humphries, D., Bermingham, L., & Reynolds, C. (2018).
884 Application of Sentinel-2A data for pasture biomass monitoring using a physically based
885 radiative transfer model. *Remote Sensing of Environment*, 218, 207-220.
886 doi:10.1016/j.rse.2018.09.028
- 887 94. Rapinel, S., Mony, C., Lecoq, L., Clément, B., Thomas, A., & Hubert-Moy, L. (2019). Evaluation
888 of Sentinel-2 time-series for mapping floodplain grassland plant communities. *Remote*
889 *Sensing of Environment*, 223, 115-129. doi:10.1016/j.rse.2019.01.018
- 890 95. Rasmussen, J., Ntakos, G., Nielsen, J., Svensgaard, J., Poulsen, R. N., & Christensen, S. (2016).
891 Are vegetation indices derived from consumer-grade cameras mounted on UAVs sufficiently
892 reliable for assessing experimental plots? *European Journal of Agronomy*, 74, 75-92.
893 doi:10.1016/j.eja.2015.11.026
- 894 96. Robinson, N., Allred, B., Jones, M., Moreno, A., Kimball, J., Naugle, D., . . . Richardson, A.
895 (2017). A Dynamic Landsat Derived Normalized Difference Vegetation Index (NDVI) Product
896 for the Conterminous United States. *Remote Sensing*, 9(8), 863. doi:10.3390/rs9080863
- 897 97. Rocchini, D., & Cade, B. S. (2008). Quantile Regression Applied to Spectral Distance
898 Decay. *IEEE Geoscience and Remote Sensing Letters*, 5(4), 640-643.
899 doi:10.1109/lgrs.2008.2001767
- 900 98. Rocchini, D., Balkenhol, N., Carter, G. A., Foody, G. M., Gillespie, T. W., He, K. S., . . . Neteler,
901 M. (2010a). Remotely sensed spectral heterogeneity as a proxy of species diversity: Recent
902 advances and open challenges. *Ecological Informatics*, 5(5), 318-329.
903 doi:10.1016/j.ecoinf.2010.06.001
- 904 99. Rocchini, D., Boyd, D. S., Féret, J., Foody, G. M., He, K. S., Lausch, A., . . . Pettorelli, N. (2015).
905 Satellite remote sensing to monitor species diversity: Potential and pitfalls. *Remote Sensing*
906 *in Ecology and Conservation*, 2(1), 25-36. doi:10.1002/rse2.9
- 907 100. Rocchini, D., Chiarucci, A., & Loiselle, S. A. (2004). Testing the spectral variation
908 hypothesis by using satellite multispectral images. *Acta Oecologica*, 26(2), 117-120.
909 doi:10.1016/j.actao.2004.03.008
- 910 101. Rocchini, D., He, K. S., Oldeland, J., Wesuls, D., & Neteler, M. (2010b). Spectral
911 variation versus species β -diversity at different spatial scales: A test in African highland
912 savannas. *Journal of Environmental Monitoring*, 12(4), 825. doi:10.1039/b921835a
- 913 102. Rodriguez-Galiano, V., Ghimire, B., Rogan, J., Chica-Olmo, M., & Rigol-Sanchez, J.
914 (2012). An assessment of the effectiveness of a random forest classifier for land-cover
915 classification. *ISPRS Journal of Photogrammetry and Remote Sensing*, 67, 93-104.
916 doi:10.1016/j.isprsjprs.2011.11.002
- 917 103. Rodwell, J. (1992) *British Plant Communities*. Volumes I-V. Cambridge University
918 Press, UK.
- 919 104. Rouse Jr, J., Haas, R. H., Schell, J. A., & Deering, D. W. (1974). Monitoring vegetation
920 systems in the Great Plains with ERTS.

- 921 105. Schweiger, A. K., Cavender-Bares, J., Townsend, P. A., Hobbie, S. E., Madritch, M. D.,
922 Wang, R., . . . Gamon, J. A. (2018). Plant spectral diversity integrates functional and
923 phylogenetic components of biodiversity and predicts ecosystem function. *Nature Ecology &*
924 *Evolution*,2(6), 976-982. doi:10.1038/s41559-018-0551-1
- 925 106. Schäfer, E., Heiskanen, J., Heikinheimo, V., & Pellikka, P. (2016). Mapping tree species
926 diversity of a tropical montane forest by unsupervised clustering of airborne imaging
927 spectroscopy data. *Ecological Indicators*,64, 49-58. doi:10.1016/j.ecolind.2015.12.026
- 928 107. Silveira, H. L., Galvão, L. S., Sanches, I. D., Sá, I. B., & Taura, T. A. (2018). Use of
929 MSI/Sentinel-2 and airborne LiDAR data for mapping vegetation and studying the
930 relationships with soil attributes in the Brazilian semi-arid region. *International Journal of*
931 *Applied Earth Observation and Geoinformation*,73, 179-190. doi:10.1016/j.jag.2018.06.016
- 932 108. Sripada, R. P., Heiniger, R. W., White, J. G., & Meijer, A. D. (2006). Aerial Color
933 Infrared Photography for Determining Early In-Season Nitrogen Requirements in
934 Corn. *Agronomy Journal*,98(4), 968. doi:10.2134/agronj2005.0200
- 935 109. Strong, C. J., Burnside, N. G., & Llewellyn, D. (2017). The potential of small-Unmanned
936 Aircraft Systems for the rapid detection of threatened unimproved grassland communities
937 using an Enhanced Normalized Difference Vegetation Index. *Plos One*,12(10).
938 doi:10.1371/journal.pone.0186193
- 939 110. Söderström, B. O., Svensson, B., Vessby, K., & Glimskär, A. (2001). Plants, insects and
940 birds in semi-natural pastures in relation to local habitat and landscape factors. *Biodiversity*
941 *& Conservation*, 10(11), 1839-1863.
- 942 111. Tadrowski, T. (2014). Accurate Mapping using Drones (UAV's). *Geoinformatics*, 17(8),
943 18.
- 944 112. Tansley, A. (1920) The Classification of Vegetation and the Concept of Development
945 *Journal of Ecology* 8: 118-149
- 946 113. Townsend, P. A., & Walsh, S. J. (2001). Remote sensing of forested wetlands:
947 application of multitemporal and multispectral satellite imagery to determine plant
948 community composition and structure in southeastern USA. *Plant Ecology*, 157(2), 129-149.
- 949 114. Tuomisto, H., Poulsen, A. D., Ruokolainen, K., Moran, R. C., Quintana, C., Celi, J., &
950 Cañas, G. (2003). Linking Floristic Patterns With Soil Heterogeneity And Satellite Imagery In
951 Ecuadorian Amazonia. *Ecological Applications*,13(2), 352-371. doi:10.1890/1051-
952 0761(2003)013[0352:lfpwsh]2.0.co;2
- 953 115. Turner, D., Lucieer, A., Malenovsky, Z., King, D., & Robinson, S. A. (2018). Assessment
954 of Antarctic moss health from multi-sensor UAS imagery with Random Forest
955 Modelling. *International Journal of Applied Earth Observation and Geoinformation*,68, 168-
956 179. doi:10.1016/j.jag.2018.01.004
- 957 116. Veettil, B. K., Ward, R. D., Quang, N. X., Trang, N. T., & Giang, T. H. (2019). Mangroves
958 of Vietnam: Historical development, current state of research and future threats. *Estuarine,*
959 *Coastal and Shelf Science*,218, 212-236. doi:10.1016/j.ecss.2018.12.021
- 960 117. Villoslada, M., Bunce, R. G., Sepp, K., Jongman, R. H., Metzger, M. J., Kull, T., . . . Leito,
961 A. (2016). A framework for habitat monitoring and climate change modelling: Construction
962 and validation of the Environmental Stratification of Estonia. *Regional Environmental*
963 *Change*,17(2), 335-349. doi:10.1007/s10113-016-1002-7
- 964 118. Villoslada, M., Ward, R. D., Bunce, R. G., Sepp, K., Kuusemets, V., & Luuk, O. (2019).
965 Country-scale mapping of ecosystem services provided by semi-natural grasslands. *Science of*
966 *The Total Environment*,661, 212-225. doi:10.1016/j.scitotenv.2019.01.174
- 967 119. Visser, H., & Nijs, T. D. (2006). The Map Comparison Kit. *Environmental Modelling &*
968 *Software*,21(3), 346-358. doi:10.1016/j.envsoft.2004.11.013
- 969 120. Wang, R., Gamon, J. A., Cavender-Bares, J., Townsend, P. A., & Zygielbaum, A. I.
970 (2018). The spatial sensitivity of the spectral diversity-biodiversity relationship: An
971 experimental test in a prairie grassland. *Ecological Applications*,28(2), 541-556.
972 doi:10.1002/eap.1669

- 973 121. Wang, D., Xin, X., Shao, Q., Brolly, M., Zhu, Z., & Chen, J. (2017). Modeling
974 Aboveground Biomass in Hulunber Grassland Ecosystem by Using Unmanned Aerial Vehicle
975 Discrete Lidar. *Sensors*,17(12), 180. doi:10.3390/s17010180
- 976 122. Ward, R. (2012). *Landscape and ecological modelling: Development of a plant
977 community prediction tool for Estonian coastal wetlands* (Doctoral dissertation, University of
978 Brighton).
- 979 123. Ward, R. D., Burnside, N. G., Joyce, C. B., & Sepp, K. (2013). The use of medium point
980 density LiDAR elevation data to determine plant community types in Baltic coastal
981 wetlands. *Ecological Indicators*,33, 96-104. doi:10.1016/j.ecolind.2012.08.016
- 982 124. Ward, R. D., Burnside, N. G., Joyce, C. B., & Sepp, K. (2016a). Importance of
983 Microtopography in Determining Plant Community Distribution in Baltic Coastal
984 Wetlands. *Journal of Coastal Research*,321, 1062-1070. doi:10.2112/jcoastres-d-15-00065.1
- 985 125. Ward, R. D., Burnside, N. G., Joyce, C. B., Sepp, K., & Teasdale, P. A. (2016b).
986 Improved modelling of the impacts of sea level rise on coastal wetland plant
987 communities. *Hydrobiologia*,774(1), 203-216. doi:10.1007/s10750-015-2374-2
- 988 126. Ward, R. D., Teasdale, P. A., Burnside, N. G., Joyce, C. B., & Sepp, K. (2014). Recent
989 rates of sedimentation on irregularly flooded Boreal Baltic coastal wetlands: Responses to
990 recent changes in sea level. *Geomorphology*,217, 61-72.
991 doi:10.1016/j.geomorph.2014.03.045
- 992 127. Westoby, M., Brasington, J., Glasser, N., Hambrey, M., & Reynolds, J. (2012).
993 'Structure-from-Motion' photogrammetry: A low-cost, effective tool for geoscience
994 applications. *Geomorphology*,179, 300-314. doi:10.1016/j.geomorph.2012.08.021
- 995 128. Wu, C., Niu, Z., Tang, Q., & Huang, W. (2008). Estimating chlorophyll content from
996 hyperspectral vegetation indices: Modeling and validation. *Agricultural and Forest
997 Meteorology*,148(8-9), 1230-1241. doi:10.1016/j.agrformet.2008.03.005
- 998 129. Xie, Q., Dash, J., Huang, W., Peng, D., Qin, Q., Mortimer, H., . . . Ye, H. (2018).
999 Vegetation Indices Combining the Red and Red-Edge Spectral Information for Leaf Area Index
1000 Retrieval. *IEEE Journal of Selected Topics in Applied Earth Observations and Remote
1001 Sensing*,11(5), 1482-1493. doi:10.1109/jstars.2018.2813281
- 1002 130. Xue, J., & Su, B. (2017). Significant Remote Sensing Vegetation Indices: A Review of
1003 Developments and Applications. *Journal of Sensors*,2017, 1-17. doi:10.1155/2017/1353691
- 1004 131. Yesilnacar, E., & Süzen, M. L. (2006). A land-cover classification for landslide
1005 susceptibility mapping by using feature components. *International Journal of Remote
1006 Sensing*, 27(2), 253-275. doi:10.1080/0143116050030042
- 1007 132. Zabalza, J., Ren, J., Yang, M., Zhang, Y., Wang, J., Marshall, S., & Han, J. (2014). Novel
1008 Folded-PCA for improved feature extraction and data reduction with hyperspectral imaging
1009 and SAR in remote sensing. *ISPRS Journal of Photogrammetry and Remote Sensing*,93, 112-
1010 122. doi:10.1016/j.isprsjprs.2014.04.006
- 1011 133. Zulian, G., Stange, E., Woods, H., Carvalho, L., Dick, J., Andrews, C., . . . Viinikka, A.
1012 (2018). Practical application of spatial ecosystem service models to aid decision
1013 support. *Ecosystem Services*,29, 465-480. doi:10.1016/j.ecoser.2017.11.005
- 1014 -